



How many ferrocene units of multi-ferrocenyl complexes can react with the electrode?

Ruo-Xuan Gao¹ · Yuan-Yuan Gao¹ · Rui-Jun Xie¹ · Li-Min Han¹

Received: 14 May 2019 / Accepted: 3 September 2019 / Published online: 10 September 2019
© Institute of Chemistry, Slovak Academy of Sciences 2019

Abstract

Ferrocenylcarboxylic acid Fe, Co, and Ni complexes were synthesized as model complexes to investigate how many ferrocene units of multi-ferrocenyl system can react with the electrode. The molecular structures of model complexes were characterized by X-ray single-crystal diffraction, the diffusion coefficient of the complexes and ferrocene was determined by the diffusion-ordered spectroscopy and Einstein–Stokes equation, the electrode reaction numbers of ferrocene units were determined by cyclic voltammetry and the Randles–Sevcik equation. A model of electrode reaction of multi-ferrocenyl system was proposed in this paper, which was used to explore how many ferrocene units of multi-ferrocenyl complexes can react with the electrode.

Keywords Ferrocene · Charge transfer · Complex · Electrode reaction model

List of symbols

i_p	Current maximum (A)
n	Number of electrons transferred in the redox process
A	Electrode area (cm ²)
F	Faraday constant
D	Diffusion coefficient (cm ² s ⁻¹)
C	Concentration (mol cm ⁻³)
ν	Scan rate (V s ⁻¹)
R	Gas constant
T	Temperature (°C)
K	Boltzmann constant

Greek letters

α	Molecular radius (Å)
η	Solution viscosity (m Pa s)

Introduction

Multi-ferrocenyl system has been extensively used as a model system for investigating intra-molecular charge transfer processes, the research topics are generally focused on the electrochemical communication and charge transfer numbers about the ferrocene units (Li et al. 2016; Chandrasekhar and Thirumoorthi 2008; Kuhnert et al. 2009; Liu et al. 2002; Collins and Pettit 1967). Hence, more and more multi-ferrocenyl model molecules have been synthesized for researching their charge transfer processes and conforming intra-molecular charge transfer numbers (Wang et al. 2008; Wu et al. 2013a, b; Pinel et al. 2015; Turlington et al. 2016). For example, the cyclic voltammetry of (ortho, meta, para) diferrocenylbenzene displays two pairs of redox waves, which involve two steps of one-electron charge transfer processes (Patoux et al. 1997; Meyer et al. 2015). The cyclic voltammetry of 1,2,4-triferrocenylbenzene displays two pairs of redox waves, one is one-electron charge transfer process, the other is two-electron charge transfer process (Luo et al. 2010). However, the cyclic voltammetry of 1,3,5-triferrocenylbenzene only takes on one pair of redox waves, it is a one-step three-electron charge transfer process (Iyoda et al. 1997). The cyclic voltammetry of tetraferrocenylbenzene has three pairs of redox waves, which involve two one-step one-electron processes and a one-step two-electron process (Xie et al. 2015). The cyclic voltammetry of hexaferrocenylbenzene also has three pairs of redox waves

Electronic supplementary material The online version of this article (<https://doi.org/10.1007/s11696-019-00922-7>) contains supplementary material, which is available to authorized users.

✉ Li-Min Han
hanlimin_442@hotmail.com

¹ Chemical Engineering College, Inner Mongolia University of Technology, Hohhot 010010, China

with a one-step one-electron process, followed by a one-step two-electron process, and a one-step three-electron electrode reaction process at last (Yu et al. 2006).

For more large multi-ferrocenyl system (Li et al. 2016; Tan et al. 2018; Villalonga et al. 2013; Morita et al. 2008), the cyclic voltammetry of ferrocenyldendrimer with n ferrocene units takes on only one pair of redox waves, it means its electrode reaction is one-step n electrons process (Beer et al. 1991; Didier 2011). The cyclic voltammetry of ferrocenyl-modified polystyrene latex particle with more than 4.5×10^8 ferrocene units also takes on only one pair of redox waves, but the number of ferrocene units that can take part in the electrode reaction is related to the particle size (Han et al. 2007a, b). For the smaller multi-ferrocenyl model molecules, such as diferrocenylbenzenes, triferrocenylbenzenes, and hexaferrocenylbenzene, their electrode reaction processes are unambiguous (Deng et al. 2008; Bai et al. 2006), but for the larger multi-ferrocenyl molecule, how many ferrocene units can react with the electrode still is a scientific problem (Han et al. 2007a, b; Esmā et al. 2017). In this paper, we synthesized three ferrocenylcarboxylic acid Fe, Co, Ni complexes as model compounds to investigate the charge transfer numbers in their electrode reaction processes.

Experimental

Chemicals

All chemicals were commercially available and used without purification. Ferrocenylcarboxylic acid and $\text{Co}(\text{NO}_3)_2 \cdot 6\text{H}_2\text{O}$ were purchased from Shanghai Aladdin Biological Technology Co., Ltd. (Shanghai, China). $\text{FeCl}_2 \cdot 4\text{H}_2\text{O}$ and $\text{Ni}(\text{NO}_3)_2 \cdot 6\text{H}_2\text{O}$ were purchased from Sinopharm Chemical Reagent Co., Ltd. (Shanghai, China).

Apparatus

Elemental analyses (C, O and H) were performed using an Elementar var EL Cube-type analyzer. FT-IR spectra were measured on a PerkinElmer FT-IR spectrum. Cyclic voltammetry were performed on a CHI 760C electrochemical analyzer. The working electrode was a platinum electrode, the reference electrode was an Ag/AgCl (3.0 M KCl), and the counter electrode was a platinum wire. Oxygen was purged from the one-compartment cell before each electrochemical run. The molecular structures of ferrocenylcarboxylic acid Fe, Co, Ni complexes were obtained by a Bruker D8 VENTURE diffractometer. DOSY-NMR spectra in mixer of THF-*d*8 and CD_3CN were recorded with an Agilent 500 MHz DD2 spectrometer.

Preparation of complexes (1)–(3)

$[\text{Fe}_3(\mu_3\text{-O})(\text{FcCOO})_6(\text{CH}_3\text{OH})_3] \cdot 2\text{CH}_3\text{OH}$ (1): FcCOOH (0.0991 g; 0.431 mmol) and $\text{FeCl}_2 \cdot 4\text{H}_2\text{O}$ (0.0546 g; 0.431 mmol) were dissolved in MeOH (15 mL) in a flask, then the reaction mixture was stirred and refluxed for 3 h. The resulting dark yellow solution was cooled to room temperature and filtered. The filtrate was allowed to stand at room temperature for slow evaporation. Good-quality black green crystals were obtained after several days. Anal. Calcd. (%) for $\text{C}_{71}\text{H}_{74}\text{Fe}_9\text{O}_{18}$: C, 49.64; H, 4.34; O, 16.76. Found (%): C, 49.21; H, 4.52; O, 17.11. IR: 1561(s, γ_{as} COO), 1471(vs, γ_{s} C–C Cp), 1385(vs, γ_{s} COO), 1353.7(s, γ_{as} C–H), 1193.5(m, $\delta_{\text{C-H}}$), 1025.4(m, $\delta_{\text{C-H}}$), 1002(w, $\delta_{\text{C-H}}$), 818.24(m, $\gamma_{\text{C-H}}$).

$[\text{Co}_3(\mu_3\text{-O})(\text{FcCOOH})_6(\text{CH}_3\text{OH})_3] \cdot 2\text{CH}_3\text{OH}$ (2): the complex (2) was prepared in a manner analogous to that used to prepare complex (1). $\text{Co}(\text{NO}_3)_2 \cdot 6\text{H}_2\text{O}$ (0.1253 g; 0.431 mmol) reacted with FcCOOH (0.0991 g; 0.431 mmol), black green crystals complex (2) was obtained. Anal. Calcd (%) for $\text{C}_{71}\text{H}_{73}\text{Co}_3\text{Fe}_6\text{O}_{18}$: C, 49.40; H, 4.26; O, 16.68. Found (%): C, 49.02; H, 4.49; O, 17.03. IR: 1566.28(s, γ_{as} COO), 1474.05(vs, γ_{s} C–C Cp), 1384.79(vs, γ_{s} COO), 1355.04(s, γ_{as} C–H), 1191.4(m, $\delta_{\text{C-H}}$), 1105.12(m, $\delta_{\text{C-H}}$), 1027.77(w, $\delta_{\text{C-H}}$), 822.48(m, $\gamma_{\text{C-H}}$).

$[\text{Ni}_3(\mu_3\text{-O})(\text{FcCOOH})_6(\text{CH}_3\text{OH})_3] \cdot 2\text{CH}_3\text{OH}$ (3): the complex (3) was prepared in a manner analogous to that used to prepare complex (1). $\text{Ni}(\text{NO}_3)_2 \cdot 6\text{H}_2\text{O}$ (0.1257 g; 0.431 mmol) reacted with FcCOOH (0.0991 g; 0.431 mmol), black green crystals complex (3) was obtained. Anal. Calcd (%) for $\text{C}_{71}\text{H}_{74}\text{Ni}_3\text{Fe}_6\text{O}_{18}$: C, 49.39; H, 4.32; O, 16.68. Found (%): C, 48.99; H, 4.52; O, 17.04. IR: 1566.28(s, γ_{as} COO), 1471.07(vs, γ_{s} C–C Cp), 1384.79(vs, γ_{s} COO), 1355.04(s, γ_{as} C–H), 1191.4(m, $\delta_{\text{C-H}}$), 1102.15(m, $\delta_{\text{C-H}}$), 1000.99(w, $\delta_{\text{C-H}}$), 816.53(m, $\gamma_{\text{C-H}}$).

Structure determination

Single-crystal X-ray diffraction measurements were carried out on a Bruker D8 VENTURE diffractometer. The diffraction data were collected with $\text{MoK}\alpha$ radiation ($\lambda = 0.71073 \text{ \AA}$). The structure was solved by direct technique using SHELXS-97 program (Sheldrick 1997a, b) and refined with SHELXL-97 by full matrix least-squares refinement on F^2 (Sheldrick 1997a, b). Crystal data and details of the data collection and the structure refinements are given in Table S1.

Results and discussion

Crystal structural description

The complexes (1), (2), and (3) show the same configuration, and the selected bond lengths and bond angles are listed in

Table S2, S3, and S4, respectively. The molecular structure and coordination polyhedron of complex **(1)** are shown in Fig. 1.

The result of X-ray diffraction analysis reveals that the complex **(1)**, with a formula of $C_{71}H_{74}Fe_9O_{18}$, crystallizes in the triclinic system, space group $P-1$. The complex unit consists of three Fe atoms, deposited in a triangular arrangement and bridged by a central μ_3 -oxido atom O(1) in the plane of the Fe-centers (Fig. 1a). The Fe(1)–Fe(2), Fe(1)–Fe(3), Fe(2)–Fe(3) distances are 3.283, 3.282, and 3.294 Å, respectively, and the average angle of Fe–O(μ_3 -O)–Fe is 120.005° . Three iron atoms are situated in the corners of an equilateral triangle structure. The dihedral angle of Fe(1)–O(1)–Fe(2) plane and Fe(1)–O(1)–Fe(3) plane is 0.122° , which indicates that the two planes are nearly in the same plane. The average angle of O(μ_3 -O)–Fe–O(CH₃OH) is 177.356° which is close to a straight line. The Fe–O(carboxylate) bond average

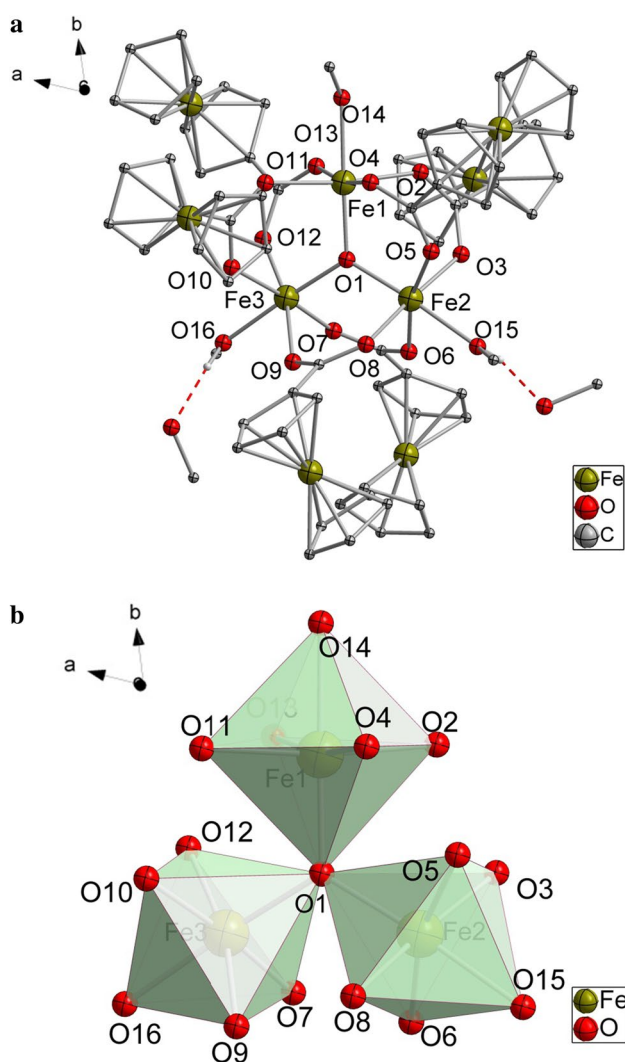


Fig. 1 a Molecular structure of complex **(1)**. All hydrogen atoms are omitted for clarity. b Coordination polyhedron of complex **(1)**

distance is 2.011 Å, which is longer than the Fe–O (μ_3 -O) bond average distance (1.898 Å) and shorter than the Fe–O (CH₃OH) bond average distance (2.0770 Å). There is a little difference from the similar structures in the literature (Silvia et al. 2011). There are no intermolecular hydrogen bonds. Two solvated methanol molecules are located near two coordinated methanol molecules from the inner sphere of the complex and form hydrogen bonds with them.

The bridging FcCOO[–] ligands are placed above and below the plane defined by the three Fe atoms in a pseudo-octahedral arrangement as a result of the local symmetry (Fig. 1b). The methanol molecules bound to the three Fe atoms at the periphery of the structure. Edges of the Fe₃ triangle are connected by μ_2 -FcCOO[–] ions and each Fe atom occupies the center of a distorted octahedron, consisting of μ_3 -O, four carboxylate oxygens and a terminal methanol oxygen atom to complete the coordination. Six ferrocenyls arraying around Fe connected to μ_3 -O basically reach spherical state in three-dimensional direction, and they are evenly distributed in entire spheroid. The complexes **(2)** and **(3)** have the same molecular structures as complex **(1)** except hydrogen bonds shown in Fig. 2.

Electrochemistry

Cyclic voltammetry (CV) of ferrocene and complexes **(1)**–**(3)** with concentration of 0.5 mmol L^{-1} was performed in mixer of tetrahydrofuran and acetonitrile (v:v 1:1). All measurements were carried out on a CHI 760C electrochemical analyzer, the working electrode was platinum electrode with diameter of 2.0 mm, which was polished with 50 μm and 10 nm alumina before each run. The reference electrode was Ag|AgCl electrode. The counter electrode was platinum wire. Supporting electrolyte was tetrabutylammonium hexafluorophosphate (0.05 mol L^{-1}). The cyclic voltammograms of ferrocene and complexes **(1)**–**(3)** are shown in Fig. 3.

Through comparing the solubility of the ferrocene and complexes **(1)**–**(3)** in conventional solvents (see Table S5), the mixer of tetrahydrofuran and acetonitrile (v:v 1:1) was selected as a solvent. Selecting tetrahydrofuran as solvents was due to its excellent solubility for ferrocene and complexes **(1)**–**(3)**, the addition of acetonitrile was to reduce the viscosity and electrochemical impedance.

The ratio of anodic and cathodic peak current of ferrocene and complexes **(1)**–**(3)** was about 1, and they seemed to be electrochemical reversible. But the potential difference of complexes **(1)**–**(3)** was about 0.21 V, they seemed to be quasi-reversible, which might be ascribed to lower coefficient or by solution impedance (Bard and Faulkner 2001). Herein, the electrode reaction of complexes **(1)**–**(3)** was approximately treated as reversible.

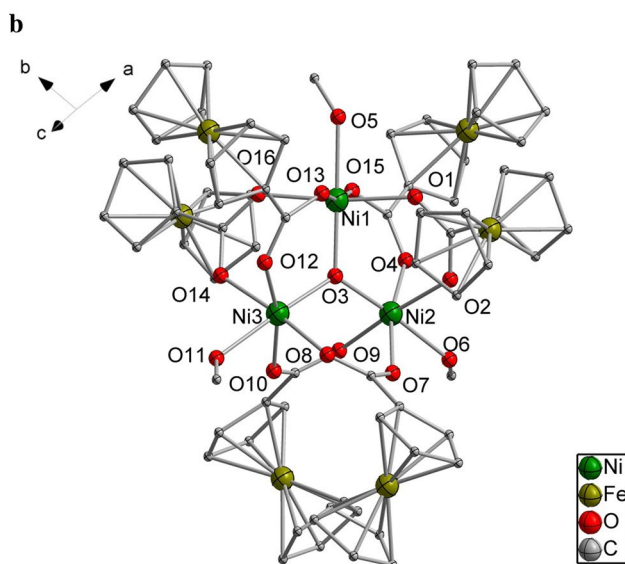
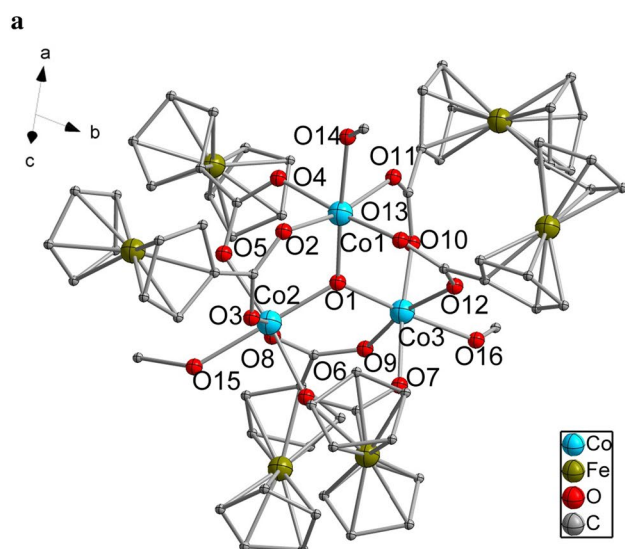


Fig. 2 **a** Molecular structure of complex (2). All hydrogen atoms are omitted for clarity. **b** Molecular structure of complex (3). All hydrogen atoms are omitted for clarity

The complex (1) was electroactive in the potential domain from 0.25 to 1.4 V, and the anodic and cathodic peak potential of complexes (1) did not vary with the scan rate, shown in Fig. 4a, the peak current increased with the increase of scanning rate. The anodic peak currents i_p were proportional to the square-root of the potential scan rate ν , as shown in the inset of Fig. 4b, indicating a diffusion-controlled process (Gao and Chen 2005).

Determination of how many ferrocene units can react with the electrode

For large spherical molecules, all redox active moieties can not simultaneously contact with the electrode (Jonas et al.

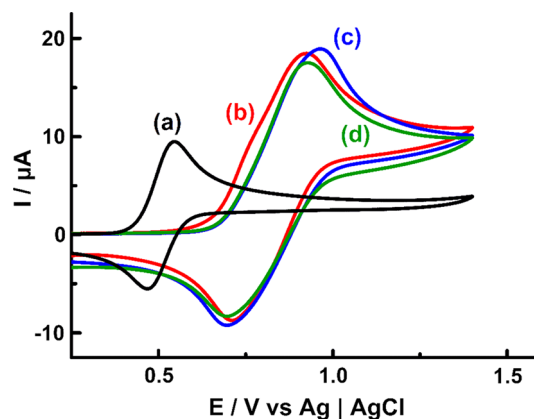


Fig. 3 The cyclic voltammograms of 0.5 mmol L⁻¹ ferrocene (a black line) and complex (1) (b red line), (2) (c blue line) and (3) (d green line) at the scan rates of $\nu = 0.1 \text{ V s}^{-1}$

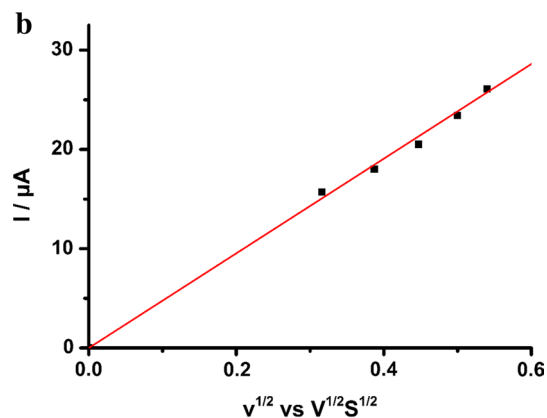
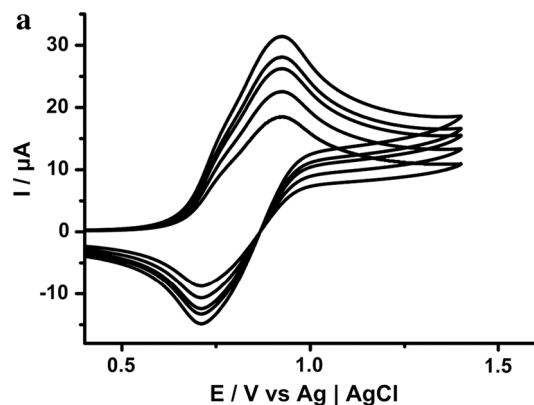


Fig. 4 **a** The cyclic voltammograms of 0.5 mmol L⁻¹ complex (1) at platinum electrode at the scan rates of $\nu = 0.1 \text{ V s}^{-1}$, 0.15 V s^{-1} , 0.2 V s^{-1} , 0.25 V s^{-1} and 0.3 V s^{-1} . **b** Variation of the peak currents of the complex (1) with the square-root of the potential scan rate. The linear proportionality implies that the peak currents should be controlled by the diffusion of complex (1)

2002). How many ferrocene units can react with the electrode? Because the electrode reaction process of ferrocene is reversible (see Fig. 3), the charge transfer number of ferrocene can be calculated by Randles–Sevcik equation (Bard and Faulkner 2001).

$$i_p = 0.4463nFAC \left(\frac{nFvD}{RT} \right)^{\frac{1}{2}} \quad (1)$$

At 25 °C, the Eq. (1) can be expressed as

$$i_p = (2.69 \times 10^5) n^{\frac{3}{2}} A D^{\frac{1}{2}} C v^{\frac{1}{2}} \quad (2)$$

For Eq. (2), the i_p , C , A and v can be known value, diffusion coefficient D can be estimated by the Einstein–Stokes Equation (Atkins 1998).

$$D = \frac{KT}{6\pi\alpha\eta} \quad (3)$$

where, T is absolute temperature, α can be obtained by the crystal structure, η is 0.36 m Pa s, when 298 K, measured using Ubbelohde viscometer. The diffusion coefficient D of the ferrocene and complex (1)–(3) in tetrahydrofuran and acetonitrile solution are calculated by Eq. (3), which are $D_{\text{ferrocene}} = 2.26 \times 10^{-5} \text{ cm}^2/\text{s}$, $D_{\text{complex(1)}} = 7.09 \times 10^{-6} \text{ cm}^2/\text{s}$, $D_{\text{complex(2)}} = 7.08 \times 10^{-6} \text{ cm}^2/\text{s}$ and $D_{\text{complex(3)}} = 7.09 \times 10^{-6} \text{ cm}^2/\text{s}$, respectively.

The i_p value of ferrocene is 8.05 μA (see Fig. 3a), take the i_p value, electrode area A , calculated diffusion coefficient D , concentration C and scan rate v into the Eq. (2), the calculated electrode reaction number of ferrocene (n) is about $1.18 \approx 1$. The result validates the effectiveness of the calculation approach. Hence, we can estimate electrode reaction numbers of ferrocene (n) of the complex (1)–(3) by this way.

The complex (1)–(3) bearing six ferrocenyls exhibits only one redox process in the CV, which indicates that there is no electronic communication about the ferrocenyl units. The i_p values of complex (1), (2) and (3) are 15.87 μA , 16.12 μA and 15.53 μA , taking these i_p values into the Eq. (2), electrode reaction numbers of ferrocene in the complex (1)–(3) are $n_1 = 2.71$, $n_2 = 2.74$ and $n_3 = 2.67$, respectively. They are not equal to 6, this means, only a part of ferrocene units in the complex (1)–(3) react with the electrode. The thickness of electrode reaction can be estimated as 1.0 nm via the molecular crystal data of the complex (1)–(3).

Diffusion-Ordered Spectroscopy Nuclear Magnetic Resonance (DOSY-NMR) can measure the diffusion coefficient of the sample in solution, which was used to verify the accuracy of the results estimated by the Einstein–Stokes equation. DOSY-NMR was conducted with an Agilent standard bipolar stimulated echo (BPPSET) pulse sequence. 15 BPPSET spectra with 512 data points were collected for each DOSY experiment (Ma et al. 2019). The tests were prepared in 10 mmol L⁻¹ solution of the ferrocene and

complex (1)–(3) of tetrahydrofuran and acetonitrile (v:v 1:1) using 5 mm NMR tubes, with the temperature of 298 K. The diffusion coefficients of complex results are as follows, $D'_{\text{ferrocene}} = 4.1 \times 10^{-5} \text{ cm}^2/\text{s}$, $D'_{\text{complex(1)}} = 6.9 \times 10^{-6} \text{ cm}^2/\text{s}$, $D'_{\text{complex(2)}} = 6.9 \times 10^{-6} \text{ cm}^2/\text{s}$, $D'_{\text{complex(3)}} = 6.6 \times 10^{-6} \text{ cm}^2/\text{s}$ (see Fig. 5). Especially, the diffusion coefficients of complexes (1)–(3) were similar, and they were also similar to the calculation result estimated by the Einstein–Stokes equation. The calculating charge transfer numbers of four compounds with the DOSY test values are as follows, $n'_{\text{ferrocene}} = 0.96$, $n'_{\text{complex(1)}} = 2.73$, $n'_{\text{complex(2)}} = 2.76$ and $n'_{\text{complex(3)}} = 2.56$. The results are similar to the calculation results, and the differences between them are $\Delta n_{\text{ferrocene}} = 0.22$, $\Delta n_{\text{complex(1)}} = 0.02$, $\Delta n_{\text{complex(2)}} = 0.02$, and $\Delta n_{\text{complex(3)}} = 0.11$, proving the accuracy of the calculation results. There are some reasonable errors due to the test concentration.

We propose an electrode reaction model for spherical multi-ferrocene system (see Fig. 6). For a large spherical multi-ferrocene system, the ferrocene can not react with the electrode simultaneously, only a part of ferrocene reacts with the electrode. Metal ions located at the coordination center, such as Fe, Co, and Ni do not participate in the reflection in the model established in this paper, whatever from the perspective of the cyclic voltammograms or the number of electrons transferred in the redox process. The react number can be estimated by the Randles–Sevcik equation and the molecular crystal structure data.

Conclusions

In summary, complex (1)–(3) were successfully synthesized and their molecular structures were characterized by X-ray single-crystal diffraction. By comparing the cyclic voltammetry of ferrocene and complexes (1)–(3), estimating the diffusion coefficient of complexes (1)–(3) and ferrocene by diffusion-ordered spectroscopy (DOSY) and Einstein–Stokes equation, calculating the electrode reaction numbers of ferrocene of complex (1)–(3), an electrode reaction model of spherical multi-ferrocenyl system was proposed. If the diameter of a spherical multi-ferrocenyl system is larger than about 1 nm, the ferrocene units of the spherical multi-ferrocenyl system can not react with electrode completely. This model can be used to predict how many ferrocene units of the spherical multi-ferrocenyl system react with the electrode.

Acknowledgements We are grateful to the Program for New Century Excellent Talents in University (NCET-08-858) and the Natural Science Foundation of China (NSFC-21462029).

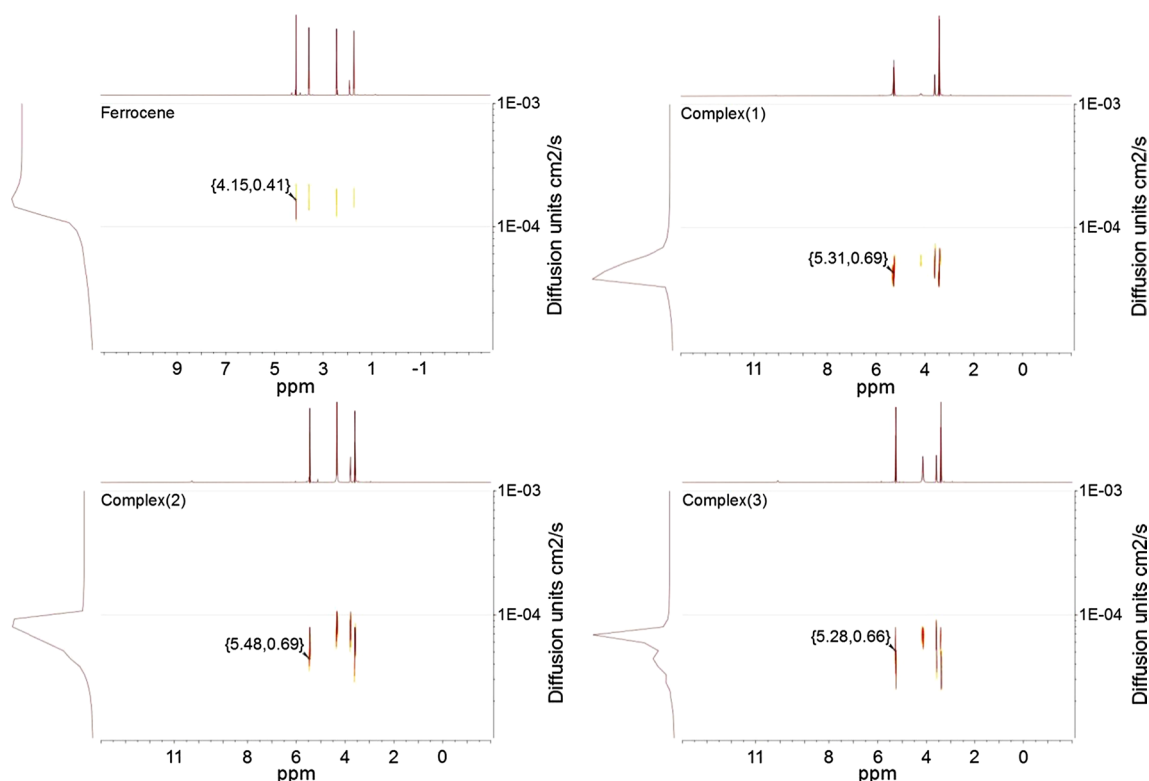


Fig. 5 DOSY-NMR of 10 mmol L⁻¹ ferrocene and complex (1)–(3) (500 MHz, THF-*d*8 and CD₃CN, 298 K)

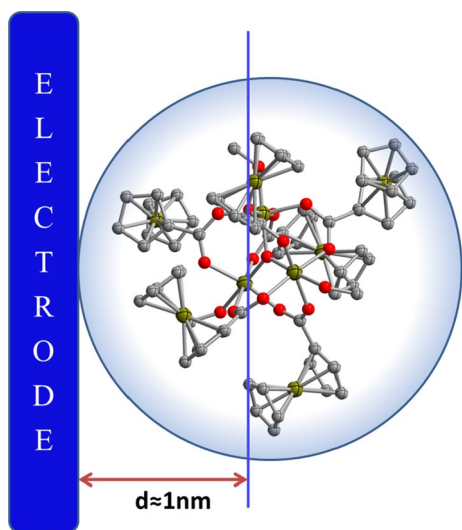


Fig. 6 Contact between ferrocene complex model and electrodes

References

- Atkins PW (1998) Physical chemistry, 6th edn. Oxford University Press, Oxford
- Bai Y, Zhang B, Duan C, Dang D, Meng Q (2006) Anion induced binding electrochemical signal transduction in ferrocenyl benzolimidazolium podands. *New J Chem* 30:266–271. <https://doi.org/10.1039/b508173d>
- Bard AJ, Faulkner LR (2001) Electrochemical methods fundamentals and applications. Department of Chemistry and Biochemistry University of Texas at Austin, New York
- Beer PD, Tite EL, Lbbotsonb A (1991) Multi redox-active macrocyclic host molecules containing multiple benzo crown ether and ferrocenyl moieties that bind bipyridinium dications: syntheses, co-ordination and electrochemical properties. *J Chem Soc Dalton Trans.* <https://doi.org/10.1039/dt9910001691>
- Chandrasekhar V, Thirumoorthi R (2008) Facile, ambient temperature, double Sn–C bond cleavage: synthesis, structure, and electrochemistry of organotin and organotellurium ferrocenecarboxylates. *Eur J Inorg Chem.* <https://doi.org/10.1002/ejic.200800574>
- Collins RL, Pettit R (1967) Mössbauer studies of iron organometallic complexes—V The stable ferrocene-tetracyano ethylene charge-transfer complex. *J Inorg Nucl Chem.* [https://doi.org/10.1016/0022-1902\(67\)80054-x](https://doi.org/10.1016/0022-1902(67)80054-x)
- Deng L, Wang L, Yu H, Wang J, Dong X, Li J, Tan Q, Huo J (2008) Synthesis and electrochemical properties of phloroglucin-based ferrocenyl compounds and their application in anion recognition. *J Appl Polym Sci* 107:1539–1546. <https://doi.org/10.1002/app.27130>
- Didier A (2011) Ferrocenyl dendrimers: multi-electron redox reagents and their applications. *New J Chem* 35:764–772. <https://doi.org/10.1039/c0nj00875c>
- Esma D, Muamer D, Narkpa NJ, Mehmet S (2017) Development of novel amperometric urea biosensor based on Fc-PAMAM and MWCNT bio-nanocomposite film. *Sens Actuators B Chem* 246:920–926. <https://doi.org/10.1016/j.snb.2017.02.122>

- Gao Y, Chen J (2005) Electrocatalysis of carbon dioxide with hemin and hemin-coated latex. *J Electroanal Chem* 583:286–291. <https://doi.org/10.1016/j.jelechem.2005.06.011>
- Han J, Cai YH, Liu L, Yan CG, Li Q (2007a) Syntheses, crystal structures, and electrochemical properties of multi-ferrocenyl resorcinarenes. *Tetrahedron* 63:2275–2282. <https://doi.org/10.1016/j.tet.2006.12.073>
- Han L, Chen J, Aoki K (2007b) Size-dependent efficiency of electron transfer at suspended ferrocenyl jumbo particles. *J Electroanal Chem* 602:123–130. <https://doi.org/10.1016/j.jelechem.2006.12.009>
- Iyoda M, Kondo T, Okabe T, Matsuyama H, Sasaki S, Kuwatani Y (1997) A simple and efficient synthesis of di-, tri-, and tetraferrocenylarenes. *Chem Lett* 26:35–36. <https://doi.org/10.1246/cl.1997.35>
- Jonas IG, Kazutake T, Héctor DA (2002) Probing diffusional transport in redox-active dendrimers. *J Phys Chem B* 106:8504–8513. <https://doi.org/10.1021/jp014080k>
- Kuhnert J, Ruffer T, Ecorchard P, Bräuer B, Lan Y, Powellb AK, Lang H (2009) Reaction chemistry of 1,1'-ferrocene dicarboxylate towards M(ii) salts (M=Co, Ni, Cu): solid-state structure and electrochemical, electronic and magnetic properties of bi- and tetrametallic complexes and coordination polymers. *Dalton Trans.* <https://doi.org/10.1039/b821407g>
- Li H, Zhao F, Yue L, Li S, Xiao F (2016) Nonenzymatic electrochemical biosensor based on novel hydrophilic ferrocene-terminated hyperbranched polymer and its application in glucose detection. *Electroanalysis* 28:1003–1011. <https://doi.org/10.1002/elan.20150604>
- Liu A, Leese DN, Swarts JC, Sykes AG (2002) Reduction of *Escherichia coli* ribonucleotide reductase subunit R2 with eight water-soluble ferrocene derivatives. *Inorg Chim Acta.* [https://doi.org/10.1016/s0020-1693\(02\)01102-7](https://doi.org/10.1016/s0020-1693(02)01102-7)
- Luo M, Han L, Suo Q (2010) Synthesis and electrochemistry of 1,2,4-triferrocenylbenzene. *Asian J Chem* 22:6715–6721
- Ma H, Pedersen C, Zhao Q, Lyu Z, Chang H, Qiao Y, Hou X, Wang Y (2019) NMR analysis of the Fischer–Tropsch wastewater: combination of 1D selective gradient TOCSY, 2D DOSY and qNMR. *Anal Chim Acta* 1166:21–27. <https://doi.org/10.1016/j.aca.2019.04.007>
- Meyer GJ, Hall GB, Smith ER, Sakamoto T, Lichtenberger DL, Glass RS (2015) Through space interaction between ferrocenes mediated by a thioether. *Polyhedron* 86:125–132. <https://doi.org/10.1016/j.poly.2014.06.050>
- Morita K, Sato Y, Seino T, Nishizawa S, Teramae N (2008) Fluorescence and electrochemical detection of pyrimidine/purine transversion by a ferrocenyl aminonaphthyridine derivative. *Org Biomol Chem* 6:266–268. <https://doi.org/10.1039/b716682f>
- Patoux C, Coudret C, Launay JP, Joachim C, Gourdon A (1997) Topological effects on intramolecular electron transfer via quantum interference. *Inorg Chem* 36:5037–5049
- Pinel LF, Kugel RW, Ault BS (2015) Charge-transfer complexes and photochemistry of ozone with ferrocene and *n*-butylferrocene: a UV–vis matrix-isolation study. *J Phys Chem A* 119:10272–10278. <https://doi.org/10.1021/ic970013m>
- Sheldrick GM (1997a) SHELXS-97 program for the solution of crystal structures. University of Göttingen, Göttingen
- Sheldrick GM (1997b) SHELXS-97 program for the refinement of crystal structures. University of Göttingen, Göttingen
- Silvia M, Denis P, Charles S, Liliana Z, Tatiana C, Valentina B, Valeriu R, Constantin T (2011) Biotechnological application of homo- and heterotrinary iron(III) furoates for cultivation of iron-enriched *Spirulina*. *Inorg Chim Acta* 373:167–172. <https://doi.org/10.1016/j.ica.2011.04.011>
- Tan H, Yu H, Song Y, Zhu S, Zhang B, Yao H, Guan S (2018) Non-volatile resistive memory devices based on ferrocene-terminated hyperbranched polyimide derived from different dianhydrides. *J Polym Sci Part A Polym Chem* 56:505–513. <https://doi.org/10.1002/pola.28920>
- Turlington MD, Pienkos JA, Carlton ES, Wroblewski KN, Myers AR, Trindle CO, Altun Z, Rack JJ, Wagenknecht PS (2016) Complexes with tunable intramolecular ferrocene to Ti(IV) electronic transitions: models for solid state Fe(II) to Ti(IV) charge transfer. *Inorg Chem* 55:2200–2211. <https://doi.org/10.1021/acs.inorgchem.5b02587>
- Villalonga BC, Vallianatou K, Georgakopoulos S, Steele BR, Micha SM, Levin E, Lemcoff NG (2013) Synthesis, characterisation, electronic spectra and electrochemical investigation of ferrocenyl-terminated dendrimers. *Tetrahedron* 69:3885–3895. <https://doi.org/10.1016/j.tet.2013.03.047>
- Wang MC, Li Y, Merbouh N, Yu H (2008) Thin-layer electrochemistry of ferrocenylbenzene derivatives: intramolecular electronic communication. *Electrochim Acta.* <https://doi.org/10.1016/j.electacta.2008.05.043>
- Wu S, Shao J, Kang H, Yao J, Zhong Y (2013a) Asymmetric mixed-valence complexes that consist of cyclometalated ruthenium and ferrocene: synthesis, characterization, and electronic-coupling studies. *Chem Asian J* 8:138–147. <https://doi.org/10.1002/asia.201200900>
- Wu S, Shao J, Kang H, Yao J, Zhong Y (2013b) Substituent and solvent effects on the electrochemical properties and intervalence transfer in asymmetric mixed-valent complexes consisting of cyclometalated ruthenium and ferrocene. *Chem Asian J* 8:2843–2850. <https://doi.org/10.1002/asia.201300739>
- Xie R, Han L, Zhu N, Gao Y, Hong H, Suo Q (2015) Synthesis of tetraferrocenylbenzene by cycloaddition reaction with alkyl cobalt clusters as reaction precursors. *J Coord Chem* 68:449–460. <https://doi.org/10.1080/00958972.2014.997720>
- Yu Y, Bond AD, Leonard PW, Lorenz UJ, Timofeeva TV, Vollhardt KP, Whitenera GD, Yakovenko AA (2006) Hexaferrocenylbenzene. *Chem Commun.* <https://doi.org/10.1039/b604844g>

Publisher's Note Springer Nature remains neutral with regard to jurisdictional claims in published maps and institutional affiliations.